Hindawi
Shock and Vibration
Volume 2022, Article ID 5181154, 20 pages
https://doi.org/10.1155/2022/5181154

Research Article

Study on the Influence of the Blasting of Preceding Tunnel on the Pre-Penetration Surrounding Rock in Succeeding Tunnel with Small Clear Distance

Xiankai Bao,[1] Wu Zhang,[1] Shuang Zhao ,[1] Chaoyun Yu,[1] Yongjun Lü,[2] Shurui Wang,[1] and Ning Wu[1]

[1]*School of Civil Engineering, Inner Mongolia University of Science and Technology, Baotou, Inner Mongolia 014010, China*
[2]*China Railway 20th Bureau Group Southern Engineering Co., Ltd, Guangzhou, Guangdong 510000, China*

Correspondence should be addressed to Shuang Zhao; 2019023228@stu.imust.edu.cn

Received 18 November 2021; Revised 16 May 2022; Accepted 27 June 2022; Published 1 August 2022

Academic Editor: Lutz Auersch

To study the influence of the preceding tunnel blasting on the surrounding rock in the pre-penetration area of the succeeding tunnel, combined with the actual monitoring of the Kaifeng Mountain small clear distance tunnel, the relationship between the vibration velocity and the blasting center distance was derived according to the energy attenuation law, predicted the peak velocity of particle vibration on the pre-penetration surrounding rock, came up with the conception of surrounding rock seismic wave vibration velocity ratio, obtained its change situation, and then established a numerical model to further analyze the changes in vibration velocity, plastic strain, and stress. The results show the prediction formula of peak vibration velocity obtained from theoretical analysis of vibration velocity, which can well calculate the peak vibration velocity of some unmeasurable points in tunnel engineering and provide theoretical support for actual tunnel blasting engineering. Under the same clear distance conditions, the front blasting side of surrounding rock in the pre-penetration area of the succeeding tunnel is affected by blasting vibration more than the back blasting side, and the vibration velocity decreases gradually from the arch waist⟶arch shoulder⟶arch foot⟶vault (arch bottom), and the most unfavorable section is that the blasting surface is parallel to the surrounding rock section in the pre-penetration area of the preceding tunnel. The excavation of the lower step has greater destructive force than that of the upper step; with the clear distance that gradually increases, the impact of the preceding tunnel blasting on the surrounding rock in the pre-penetration area of the succeeding tunnel becomes smaller, and D (D is the tunnel span) is the minimum safe clear distance.

1. Introduction

At present, a small clear distance tunnel is widely used because of the advantages of being convenient for overall road planning, but this type of tunnel usually has a small thickness of the middle rock wall between the two holes, so the construction is difficult. If the vibration velocity generated is too high during blasting excavation of the preceding tunnel, which will cause a very serious impact on the middle rock wall and the adjacent unexcavated succeeding tunnel surrounding rock, change the mechanical properties of surrounding rock and even change the geological structure of surrounding rock, and may easily lead to instability or destruction of the surrounding rock, therefore, it is particularly important to study the vibration velocity prediction in the blasting process of small clear distance tunnel and the influence of succeeding tunnel in the excavation process. In recent years, many scholars have done a lot of research on the energy attenuation and blasting vibration theory in the process of tunnel blasting, as well as the thickness and the range of plastic area of middle rock wall, the stress change in the surrounding rock, and the construction method in the small clear distance tunnel, and have made some achievements.

The blasting of the tunnel is bound to cause the generation, transformation, transmission, and work of energy, and this process is extremely short and may only take tens of microseconds. In addition, due to the uneven internal structure of the rock, the process of energy transmission becomes very complex. Tian et al. [1] found that the blasting vibration energy mainly comes from the explosion in the initial blasting. In the research, many experts and scholars have summarized and deduced particle vibration velocity attenuation equation [2] and blasting vibration energy attenuation equation [3] through engineering measurement and theoretical analysis. On these foundations, Yang et al. [4] identified and separated the waveform of transient unloading induced vibration from the measured vibration signals by means of amplitude spectrum analysis and low-pass filtering and summarized the corresponding attenuation law; Fei et al. and Yao et al. [5, 6] studied the energy distribution in different frequency bands, analyzed the attenuation law of energy in seismic wave propagation, and summarized relevant formulas, to describe the variation law of seismic wave energy more quantitatively; Shan et al. [7] used MATLAB software to decompose the vibration signals obtained by blasting of small clear distance tunnel with five-layer wavelet packet transform, solved the reconstructed signal and frequency band energy of each node, and studied the frequency band energy distribution characteristics of the blasting vibration signal. In addition, by fitting regression analysis of total energy, the corresponding total energy attenuation equation is put forward; Dai et al. [8] calculated the energy contained in the incident wave, reflected wave, and transmitted wave, respectively, based on the SHPB test, and summarized and studied the energy dissipation equation of the corresponding experiment; Liu et al. [9] explored the dynamic characteristics and failure modes of concrete under confining pressure through SHPB dynamic compression experiment and linearly fitted the dynamic growth coefficient (DIF) of concrete with the dynamic confining pressure growth coefficient (DIFc); Ji et al. [10] performed regression analysis on blasting test data based on Sadovsky's equation and studied the blasting vibration velocity propagation law of the surrounding rock in the middle rock in front of and behind the tunnel; Fan et al. [11] aimed at circular tunnel excavation under the condition of in situ stress transient unloading, studied the balance mechanism among surrounding rock kinetic energy, strain energy, and radial stress work, adopted the dimensional analysis method to establish the corresponding vibration velocity attenuation equation induced by the transient unloading of rock strain energy at excavation site, and analyzed the attenuation law that can induce vibration. Many of the above scholars have conducted in-depth studies on the energy form, transmission, attenuation, distribution characteristics, vibration changes, and other mechanisms and laws in the process of tunnel blasting construction and achieved fruitful research results, which provide a solid theoretical basis for exploring the influence of tunnel blasting on surrounding rock.

Many experts and scholars at home and abroad have predicted blasting vibration by various advanced technologies and algorithms and established various prediction models. Advanced even combines neural network with it. Xu et al. [12] studied the blasting flow produced by DLSOS (sublevel open stope method) in the process of ore body mining, analyzed the relationship between ore drawing point spacing and production blasting ring load, and established a back propagation neural network (BPNN) prediction model; Xu et al. [13] established PPV prediction model by combining genetic algorithm with artificial neural network and using mine underground blasting parameters and surface vibration monitoring data; Jayawardana et al. [14] analyzed the relationship between damping effect and control parameters of double-filled grooves by combining neural network and put forward the related vibration prediction model; Guo et al. [15] used genetic algorithm to build a GA-BP neural network prediction model, input the maximum single-stage explosive charge, blasting center distance, and monitoring parameters of the actual blasting project, and realized the prediction of blasting vibration speed; Wang [16] adopted the improved BP neural network algorithm and artificial forest algorithm to analyze the collected actual engineering blasting monitoring parameters and predict the blasting vibration speed and main frequency; in addition, Marilena et al. [17] analyzed 12 experimental cases and summarized the empirical correlation equations of vibration prediction, which provides an excellent basis for evaluating the attenuation of rock mass caused by rock blasting vibration; He et al. [18] carried out dimensional analysis of blasting vibration wave based on field experimental data, decomposed the blasting vibration signal by wavelet packet, researched the peak velocity equation of blasting vibration under the influence of elevation and the attenuation mechanism of energy along slope, and put forward a prediction model of blasting vibration related to its actual engineering; through theoretical analysis and numerical simulation, Jayasinghe et al. [19, 20] obtained the vibration velocity waveform of the surface particles caused by the cutting holes blasting and the ground vibration attenuation equation caused by the rock blasting, respectively; Xie et al. [21] determined the pulse function sequence of each blasting hole initiation based on the Anderson linear superposition model, used the convolution theory to calculate the superposition waveform of group hole blasting, and proposed a calculation model of vibration velocity in the vicinity of the tunnel, which can more accurately predict the intensity of blasting vibration; the above experts have done a lot of research on the prediction models of blasting vibration and made some achievements, but the theories and methods based on them are different, and different prediction models are suitable for specific practical projects, but they lack some universal applicability, so the prediction methods of blasting vibration still need further research.

There are also many scholars who have made in-depth studies on the influence of the construction process of small clear distance tunnel on the lining and surrounding rock. Wu and Jin [22] analyzed the peak vibration velocity under different conditions and determined the maximum effect position by blasting of the preceding tunnel, the reasonable clear distance of the tunnel, and the corresponding control blasting measures; Liu [23] analyzed the surrounding rock

stress, displacement, plastic area distribution, ground settlement, and other parameters after tunnel excavation under the conditions of different middle rock thicknesses and obtained the reasonable clear distance, reinforcement method, and effect of middle rock wall, through numerical model calculation; Yang et al. and Guo et al. [24, 25] studied the relationship between tunnel excavation and clear distance and found that the stress of rock wall was greatly affected by the clear distance, damage or crack propagation would occur on the front blasting side and back blasting side, the damage degree gradually decreased with the increase in clear distance, and the corresponding minimum safe clear distance is determined; Li et al. [26] simulated the stress characteristics and deformation of small clear distance tunnel structure under different excavation methods and discussed the corresponding reinforcement measures of the middle rock wall; Wang et al. [27] studied the influence law of the excavation process of under passing tunnel on the settlement deformation, vibration acceleration, and vibration velocity of the existing adjacent tunnel lining structure under the conditions of different construction methods, different sandwich thickness, and different train axle load; Guan et al. [28] established three-dimensional numerical models of square, circular, and horseshoe tunnels using the ALE algorithm of LS-DYNA software and compared and analyzed the influence of different types of tunnel distance changes, and it was found that the peak vibration velocity and tensile stress of three types of tunnels increased with the decrease in distance, among which the circular tunnel was the most affected, followed by the square tunnel and horseshoe tunnel; Yang et al. [29] found the weakest position of the preceding tunnel when the succeeding tunnel is excavating and obtained the relationship between the blasting vibration velocity of each particle and time; Jia et al. [30] studied the influence of the blasting excavation of a new tunnel on the vibration of existing adjacent tunnel lining by establishing a numerical model and analyzed the influence of different clear distances, excavation footage, and buried depth; Liu [31] studied the effect of the supporting structure of the preceding tunnel on the succeeding tunnel and the influence of the excavation of the succeeding tunnel on the surface settlement, vertical displacement, lining structure, and surrounding rock stress of the preceding tunnel and put forward the corresponding monitoring and reinforcement measures; the above domestic and foreign scholars have done a lot of research on many aspects, such as rock wall thickness, surrounding rock stress, plastic area distribution, and construction methods during the construction of small clear distance tunnel, and these studies have played an important role in realizing the smooth construction of small clear distance tunnel. The blasting of the preceding tunnel is bound to cause the stress redistribution and strain change in the middle rock wall and the pre-penetration surrounding rock of the succeeding tunnel. However, most of the current researches focus on the analysis of the stress and strain of the lining structure and the middle rock wall of the succeeding tunnel. There is a lack of research on the change law of the vibration velocity, stress, and strain of the surrounding rock of the preceding tunnel, and it should be further explored.

This article is based on the actual project of the Kaifeng Mountain small clear distance tunnel. Firstly, the relationship between the particle vibration velocity and the burst center distance is derived through the seismic wave attenuation equation and Sadovsky's empirical equation, and then, the peak velocity vibration, frequency, and other data from field monitoring and simulation result are analyzed and fitted to obtain the corresponding coefficients k, α, and β. Finally, the relationship between the vibration velocity and the blasting center distance of tunnel project is used to calculate the seismic wave velocity proportional coefficient V_r/V_0 of the surrounding rock in the pre-penetration area, the variation trend of the vibration velocity is judged, and the most unfavorable section in the process of blasting excavation is obtained. Then, the numerical model is established by the finite element software, and further, the changes in rock wall and pre-penetration surrounding rock are analyzed in the succeeding tunnel caused by blasting construction of the preceding tunnel through the vibration velocity, plastic strain, and stress changes. Finally, combined with field monitoring and theoretical derivation, the relevant laws are summarized to provide a reference for the construction design and actual construction of the small clear distance tunnel.

2. Project Overview and Vibration Monitoring Scheme

2.1. Project Overview. The Kaifeng Mountain tunnel is located in Baoji Village, Hongshan Town, Suizhou City, Hubei Province, which is a small clear distance double-hole separated tunnel in the Mazhu Expressway. The biggest difference between the two-hole separated tunnel with small distance and the single-hole tunnel is that the two holes will influence each other in the construction process, resulting in the deterioration of surrounding rock conditions. The blasting construction of the preceding tunnel will increase the vibration influence on the surrounding rock of the succeeding tunnel, which will disturb the surrounding pre-penetration rock, worsen the stress conditions of the tunnel, and even lead to the destruction and instability of the surrounding rock. The total length of the tunnel is about 1000 m, the span of the excavation section is 13.12 m, and the thickness of the middle rock wall is 9~12 m. The tunnel is spread from southeast to northwest direction. It is a double-track tunnel with a maximum buried depth of 70 m, located in hilly area, and the surrounding rock is grades IV and V, the geological conditions are complex, and the self-stability is poor. The detailed clearance section design is shown in Figure 1 (all units not shown in the figure are in cm).

The Kaifeng Mountain tunnel is constructed by upper and lower step methods and excavated by drilling and blasting method, and the smooth blasting technology is adopted, and the working faces of the two tunnels are staggered. The explosives are No. 2 rock ammonium nitrate explosive and emulsion explosive, and the blasting method is segmented delayed detonation network and the detonating electric detonator initiation. The total charge of the tunnel face blasting is 78 kg, divided into 8 delays, and the

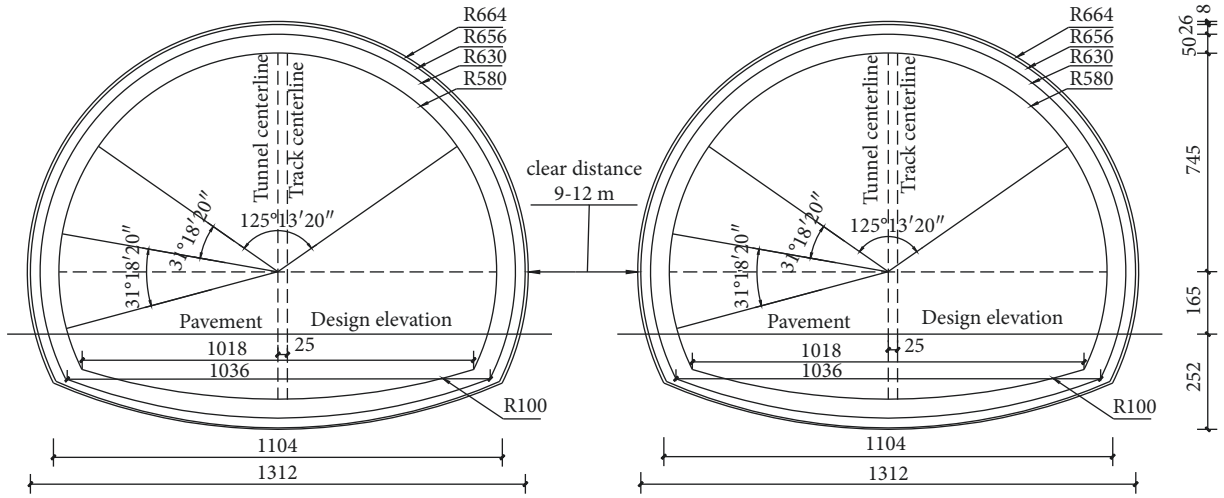

Figure 1: Design drawing of tunnel clear distance section.

maximum charge of a single stage is 15.6 kg. The diameter of cartridge is 0.032 m, the length of cartridge is 0.2 m, and the blasting hole is densely blocked with gun clay, which is composed of three components: clay, medium coarse sand, and water. The stemming length should not be less than 0.4 m, and the charge coefficient should be controlled between 75% and 80%, and intermediate holes ($1^{\#}$, $3^{\#}$, $5^{\#}$, $7^{\#}$), cutting holes ($9^{\#}$, $11^{\#}$), and peripheral holes ($13^{\#}$, $15^{\#}$) are blasted successively (Figure 2). The actual blasting effect is excellent, the residual blast hole traces are evenly distributed, the integrity of rock mass is not damaged, there is no obvious blasting crack on the excavation surface, and the blasting indexes meet the design requirements.

2.2. Monitoring Program. When the preceding tunnel is constructed, the original mechanical system of surrounding rock around the tunnel is broken, and the original stress state has changed. With the increase in excavation depth, this change will continue. To monitor the state and mechanical dynamic behavior of the pre-penetrating surrounding rock of the succeeding tunnel, the surrounding rock of the preceding tunnel and the pre-penetrating surrounding rock of the succeeding tunnel can be monitored by means of monitoring and measurement. The results can guide the construction, foresee the dangerous situation of accidents, take timely measures to prevent problems before they happen, and provide an analogy basis for the design and construction of similar projects in the future.

The main instruments used in this blasting monitoring system include horizontal and vertical velocity sensors, UBOX-20016 vibration recorder, and computer. The horizontal and vertical sensors are used to collect dynamic analog signals such as vibration velocity and vibration acceleration generated by tunnel blasting. UBOX-20016 portable data acquisition equipment is used for digital conversion and storage of the required signals, and the effective data obtained will be processed and analyzed by the computer. The specific working principle is supplemented and shown in Figure 3.

In the process of construction, it is necessary to select representative sections for the blasting vibration test. In the preceding tunnel, several vibration monitoring sensors are arranged at the arch foot and the arch waist on each cross section (Figure 4) and at different distances behind the tunnel face on the vertical section (Figure 5). The influence of blasting vibration wave on surrounding rock at different distances can be measured. The site layout is shown in Figure 6.

According to geological conditions and construction scheme of Kaifeng Mountain tunnel, combined with the corresponding measurement point layout principles and monitoring requirements, the corresponding measuring points are reasonably arranged in the direction of vertical section. Four monitoring points ($1^{\#}$, $2^{\#}$, $3^{\#}$, and $4^{\#}$) are arranged on the wall of the front blasting side of the preceding tunnel, which are 10 m, 30 m, 65 m, and 85 m away from the blasting working face, respectively, and the other two monitoring points ($5^{\#}$ and $6^{\#}$) are, respectively, arranged at 120 m from the explosion source on the back blasting side of the succeeding tunnel and 125 m from the explosion source on the front blasting side. In this study, the influence of the preceding tunnel blasting on the surrounding rock in the pre-penetration area of the succeeding tunnel is studied, since it is impossible to arrange the monitoring points inside the surrounding rock in the pre-penetration area of succeeding tunnel. Therefore, the derivation points are, respectively, arranged on the face and back blasting sides of surrounding rock in the pre-penetration area of the succeeding tunnel: taking the blasting working face as the starting point, the lines of the derivation points extend 90 m and 50 m backward and forward, respectively, and a deduction point is arranged each 10 m. The layout is shown in Figure 5.

2.3. Vibration Velocity Monitoring Results. The actual monitoring results of Kaifeng Mountain tunnel project are shown in Table 1, in which the main vibration frequency f is taken from the frequency domain waveform acquired by the sensor during the monitoring process. It can be seen from

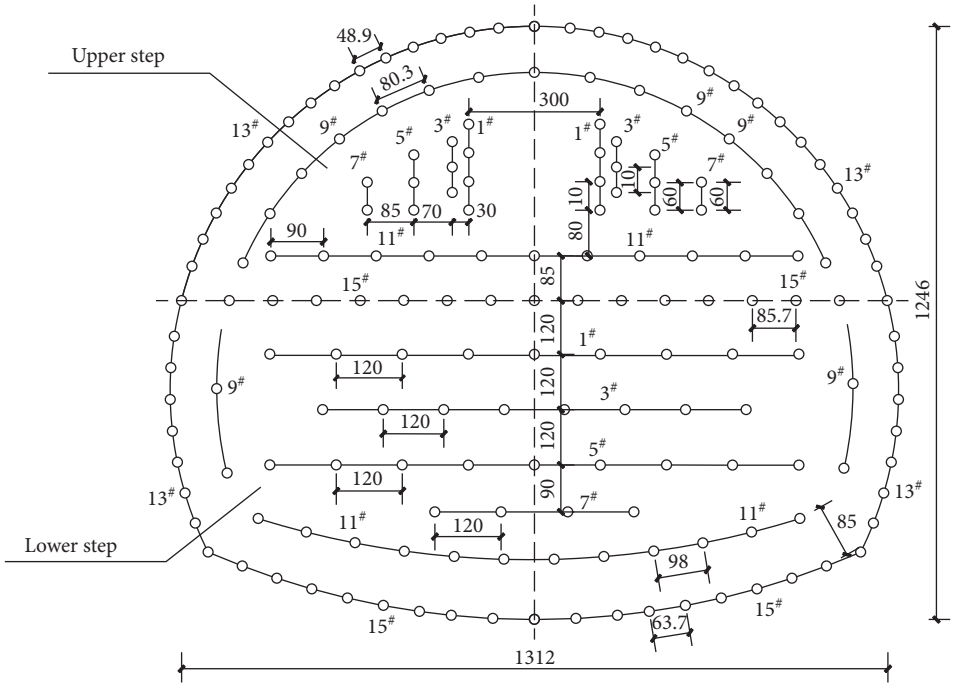

Figure 2: Layout of blasting holes.

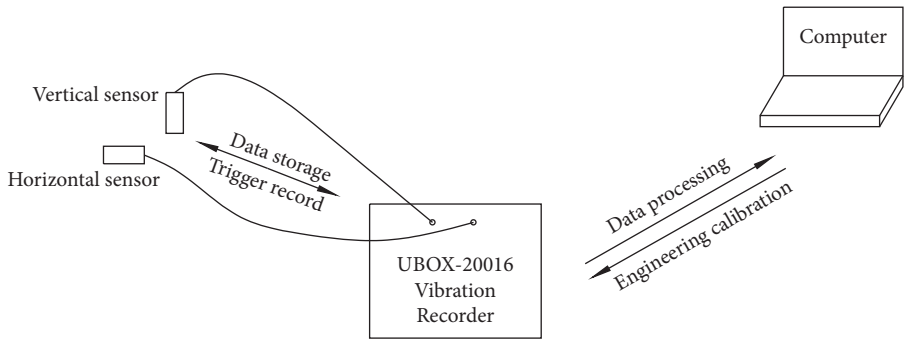

Figure 3: Schematic diagram of blasting vibration monitoring.

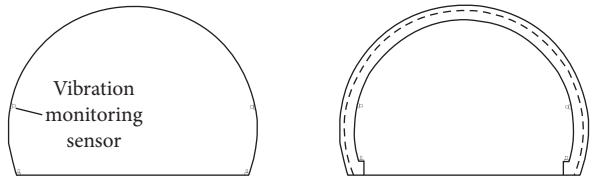

Figure 4: Layout of vibration sensor on tunnel excavation face.

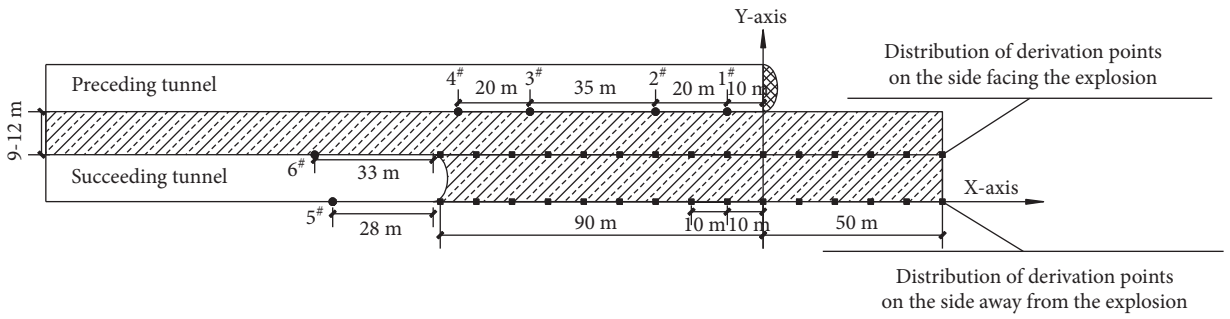

Figure 5: Schematic diagram of the layout of monitoring points and proposed points for tunnel blasting vibration.

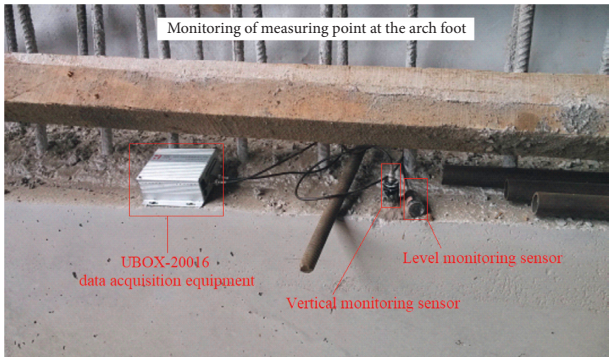

Figure 6: Field layout of instruments and sensors.

the table that the main vibration frequency range of Kaifeng Mountain small clear distance tunnel is 24.69 Hz~43.21 Hz, and the natural vibration frequency monitored by this tunnel is 3 Hz~9 Hz. There is no overlap between the two frequency ranges, and the main vibration frequency is much higher than the natural vibration frequency of the tunnel. So, there will be no resonance amplification in this blasting, and the frequency will not be considered, and only the vibration velocity will be analyzed. During the blasting excavation of this tunnel project, the maximum vibration velocity is 3.564×10^{-2} m/s, which is far less than the vibration velocity value of 12~15 cm/s specified in the national standard blasting safety regulations (GB6722-2014) (Table 2), and meets the blasting safety requirements.

3. Numerical Simulation Calculation of Blasting Excavation of Small Clear Distance Tunnel

This article takes the Kaifeng Mountain tunnel project as the background, establishes a three-dimensional numerical model using finite element software, and defines the left tunnel as a succeeding tunnel without excavation and the right tunnel as a preceding tunnel under excavation. The influence of blasting excavation of upper and lower steps of the preceding tunnel in the pre-penetration area of the succeeding tunnel is simulated under the conditions of IV type surrounding rock and different tunnel clear distances (0.15D, 0.5D, D, and 2D, while D is the tunnel span 13.12 m), and the changes in vibration velocity, plastic strain, and stress distribution of the surrounding rock in the pre-penetration area are analyzed.

3.1. Basic Dimensions and Parameters of the Model. According to existing studies [32]: the influence range of blasting excavation of tunnel is (3–5) D. Therefore, to avoid the interference caused by boundary conditions, the model takes 3D as the boundary. This article takes the tunnel clear distance of 0.15D/0.5D/D/2D to model. The span of the tunnel is 13.12 m, the height is 11 m, and the rock layers covered above the tunnel are weathered soil, strongly weathered sandstone, and carbonaceous siliceous shale with thicknesses of 9.6 m, 12.8 m, and 77.6 m, respectively. According to the influence range of rock excavation, the horizontal dimension is 120 m, the vertical height is 100 m, and the depth dimension is 60 m by calculating. The tunnel numerical calculation model is divided into 98573 nodes and 108208 units, as shown in Figure 7.

The parameters of tunnel surrounding rock and supporting materials are shown in Table 3.

3.2. Determination of Model Boundary Conditions. The shock wave generated by blasting will be reflected on the surrounding rock boundary, which will cause a big gap between the simulated calculation data and the on-site construction. Therefore, it is necessary to set the boundary conditions on the surrounding rock to simulate the continuous state of the rock in the actual project, so that the software calculation results can be more consistent with the actual situation. In the eigenvalue analysis of the model, considering the absorption of scattered wave energy by surrounding rock and its viscoelastic properties [33], the model is set as the viscoelastic boundary condition, to restore the real environmental state of rock as much as possible. Firstly, the boundary conditions of the support are established, and the reaction coefficient of elastic foundation is calculated as follows [34].

The coefficient of vertical foundation reaction is as follows:

$$k_v = k_{v0} \cdot \left(\frac{B_v}{30}\right)^{-3/4}. \quad (1)$$

The coefficient of horizontal foundation reaction is as follows:

$$k_h = k_{h_0} \cdot \left(\frac{B_h}{30}\right)^{-3/4}. \quad (2)$$

In the above equations:

$B_h = \sqrt{A_h}$, A_h = horizontal cross-sectional area of the model (m^2)

$B_v = \sqrt{A_v}$, A_v = vertical cross-sectional area of the model (m^2)

$k_{v0} = k_{h0} = \alpha \times E_0/30$, E_0 = elastic coefficient of foundation, α is a constant, and 1.0 is taken

$k_{v0} = k_{h0} = \alpha \times E_0/30$ = vertical, horizontal foundation reaction coefficient

Secondly, the reflection of wave should be considered in the dynamic analysis, and the damping constant should be manually input on each boundary of the model to generate a damper, and then, the absorption of the scattered stress wave is simulated. The viscous boundary proposed by Lysmer and Kulemeyer [35, 36]is used. The equations for calculating the damping ratio in each direction of the model required by the viscous boundary condition are as follows.

P wave is as follows:

$$C_p = \rho A \sqrt{\frac{\lambda + 2G}{\rho}} = \gamma A \sqrt{\frac{\lambda + 2G}{\gamma \cdot 9.81}} = c_p A. \quad (3)$$

S wave is as follows:

Table 1: Results of blasting vibration monitoring data.

Monitoring point	Blasting center distance R (m)	Peak vibration velocity V (m/s)	Main vibration frequency f (Hz)	Amplitude A (m)
1#	10	3.564×10^{-2}	38.64	2.076×10^{-4}
2#	30	2.689×10^{-2}	35.17	1.721×10^{-4}
3#	65	1.853×10^{-2}	33.23	1.255×10^{-4}
4#	85	1.231×10^{-2}	24.69	1.122×10^{-4}
5#	120	1.375×10^{-2}	26.13	1.184×10^{-4}
6#	125	1.397×10^{-2}	43.21	7.277×10^{-5}

Table 2: Safety allowable standard of blasting.

Tunnel category	Safety allowable vibration velocity (cm/s)		
	$f\le10$ Hz	10 Hz$<f\le$50 Hz	$f>50$ Hz
Traffic tunnel	10~12	12~15	15~20

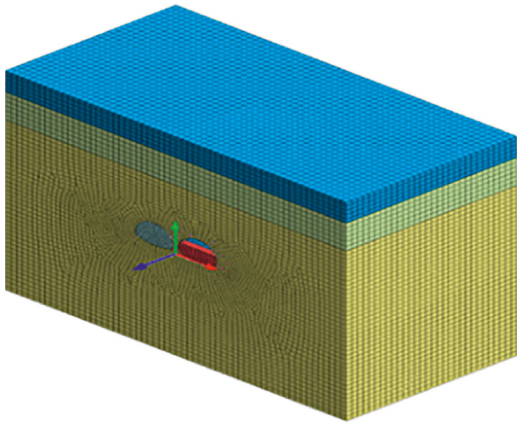

Figure 7: Tunnel model diagram.

$$C_s = \rho A\sqrt{\frac{G}{\rho}} = \gamma A\sqrt{\frac{G}{\gamma\cdot 9.81}} = c_s A. \tag{4}$$

In the above equations:

A = calculation cross section of rock and soil element (m^2)

C_p = wave velocity of P wave (m/s)

C_s = wave velocity of S wave (m/s)

E = elastic modulus (N/m^2)

G = shear elastic coefficient of rock and soil mass (N/m^2); $G = E/2(1+\nu)$

γ = the unit weight of rock and soil layer (N/m^3)

λ = elastic coefficient of model volume (N/m^2); $\lambda = \nu E/(1+\nu)(1-2\nu)$

ν = Poisson's ratio

ρ = medium density of rock and soil mass (kg/m^3)

The above equations can be used to calculate the foundation damping coefficient of each rock layer in the model, as shown in Table 4.

3.3. Determination of Blasting Load Parameters. Before the numerical calculation of tunnel blasting, it is necessary to determine the relevant parameters of blasting loading, including peak load, blasting loading waveform, and loading and unloading time. The calculation of each parameter plays an important role in the accuracy of the model and the degree of conformity with the actual project.

After blasting hole explosive, the formation of blasting stress wave load is evenly distributed on the tunnel lining, and the action direction is perpendicular to the tunnel wall [37]; according to the propagation law of wave, the form of blasting load can be simplified to the curve shown in Figure 8 [38]. $P_{\max}$ in the figure is the peak pressure on the blasting hole wall, which is related to rock properties, explosive types, charge forms, and other factors. The explosion stress wave at any point in the rock behaves as load similar to triangle, and the peak pressure decreases sharply after reaching the peak load pressure and keeps spreading forward.

Due to the functional characteristics of the software, it is difficult to establish blasting hole units one by one. Therefore, after the blasting holes are gathered together, the pressure is assumed to act vertically on the imaginary surface of the blasting, and then the normal uniform load $P_{\max}$ applied to the surrounding rock at the tunnel wall in the numerical simulation is calculated according to the empirical method. That is, in the equation mentioned in the *National Highway Institute* of the United States, the blasting load per 1 kg is as follows [39–41]:

$$P_{\det} = \frac{4.18\times10^{-7}\cdot sge\cdot V^2}{1+0.8\cdot sge}, \tag{5}$$

$$P_B = P_{de\ \ t}\left(\frac{d_c}{d_b}\right)^3. \tag{6}$$

In the above equations:

d_b = blasting hole diameter (m)

d_c = cartridge diameter (m)

P_B = blasting pressure acting on the hole wall (Pa)

$P_{de\ \ t}$ = explosion pressure per 1 kg explosive (Pa)

Table 3: Material parameters of the tunnel model.

Material	Elastic modulus E (N/m^2)	Poisson's ratio μ	Bulk density γ (N/m^3)	Cohesion C (N/m^2)	Internal friction angle φ (°)
Weathered soil	5.0×10^7	0.30	1.80×10^4	2.0×10^4	30
Weathered rock	5.0×10^8	0.30	2.30×10^4	2.0×10^4	33
Carbon silicon IV	2.4×10^9	0.33	2.10×10^4	2.6×10^5	54
Qualitative shale V	1.3×10^9	0.39	1.80×10^4	1.2×10^5	45
Spray mixing	2.8×10^{10}	0.20	2.40×10^4	—	—
Anchor	2.0×10^{11}	0.30	7.85×10^4	—	—

Table 4: Damping coefficient of model foundation (N·Sec/m).

Types of rock and soil layers	C_p	C_s
Weathered soil	3.48×10^5	1.86×10^5
Weathered rock	1.24×10^6	6.65×10^5
Carbon siliceous	2.73×10^6	1.38×10^6
Shale V	2.16×10^6	9.17×10^5

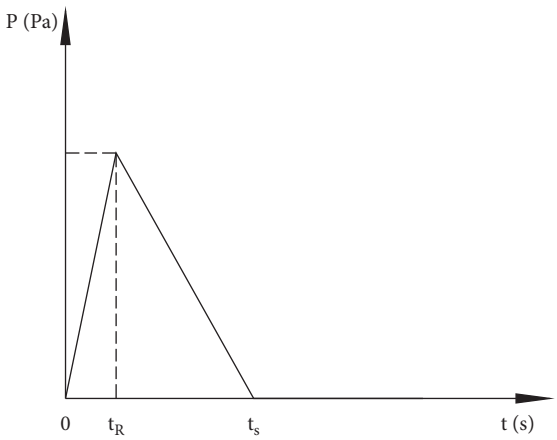

Figure 8: Blasting load waveform.

sge = specific gravity of explosives (kg/m^3)

V = blasting speed of explosive (m/s)

The loading and unloading time of blasting load can be determined by the following equation [30].

Loading rise time is as follows:

$$t_R = \frac{12\sqrt{\bar{r}^{2-\mu}}Q^{0.05}}{K}. \quad (7)$$

Total action time is as follows:

$$t_s = \frac{84\sqrt[3]{\bar{r}^{2-\mu}}Q^{0.2}}{K}. \quad (8)$$

In the above equations:

K = bulk modulus of compression (Pa); $K = E/3(1-2\mu)$

Q = blasting hole charge (kg)

$\bar{r}$ = contrast distance (the ratio of the distance r from a point to the blasting center to the radius of the blasting hole r_b)

t_R = rise time period (s)

t_s = total action time of triangle waveform (s)

μ = Poisson's ratio of rock

According to the charging structure, number of blasting sections, charging amount, and data results obtained from blasting monitoring of Kaifeng Mountain tunnel, the total action time of the blasting load applied by the numerical model is determined. It can be seen that the pressure boost time of triangular wave load is 0.008~0.012 s and the pressure relief time is 0.04~0.12 s [42]. To fit the actual construction situation as much as possible, after calculation, the numerical simulation adopts the pressure boost time of 0.008 s, the pressure relief time of 0.092 s, and the total time of 0.1 s. The explosive velocity is 3000 m/s, the specific gravity is 1.1×10^3 kg/m^3, adopt uncoupled charge, the cartridge diameter is 0.032 m, and the drilling diameter is 0.04 m. According to (5), the explosion pressure for each 1 kg can be calculated as $P_B = 1.127\times10^7$ Pa. Each excavation footage of upper step is 2 m, and the maximum charge is 13.2 kg. The blasting pressure can be calculated as 1.488×10^8 Pa through (6); each excavation footage of lower step is 2 m, the maximum charge is 26.6 kg, and the calculated blasting pressure is 2.93×10^7 Pa.

3.4. Load Results Applied by the Model. According to the parameters of rock and soil in the project, the corresponding indexes in the modeling process are set, the measuring points $1^{\#}$~$6^{\#}$ at the same position of the model (Figure 5) are arranged, the vibration velocity time-history curve (Figure 9(a)) of each measuring point is obtained, the peak vibration velocity of each measuring point is extracted, and the numerical simulation vibration data are sorted. The results are shown in Table 5. Compared with the peak value of vibration velocity obtained from the actual engineering monitoring (Figure 9(b)), so as to verify the accuracy of the model, the maximum difference between them is 3.94×10^{-3} m/s at No. 2 measuring point, and the relative error is 14.7%. The minimum value is 7.8×10^{-4} m/s at No. 3 measuring point, and the relative error is 4.21%. The average value is 8.23×10^{-4} m/s, and the average relative error is 10.4%. It can be seen that the error between the peak value of numerical simulation vibration velocity and the peak value of actual monitoring vibration velocity is slight, which indicates that the parameters used in the finite element model are properly selected, and the model can better simulate the reality of the construction site.

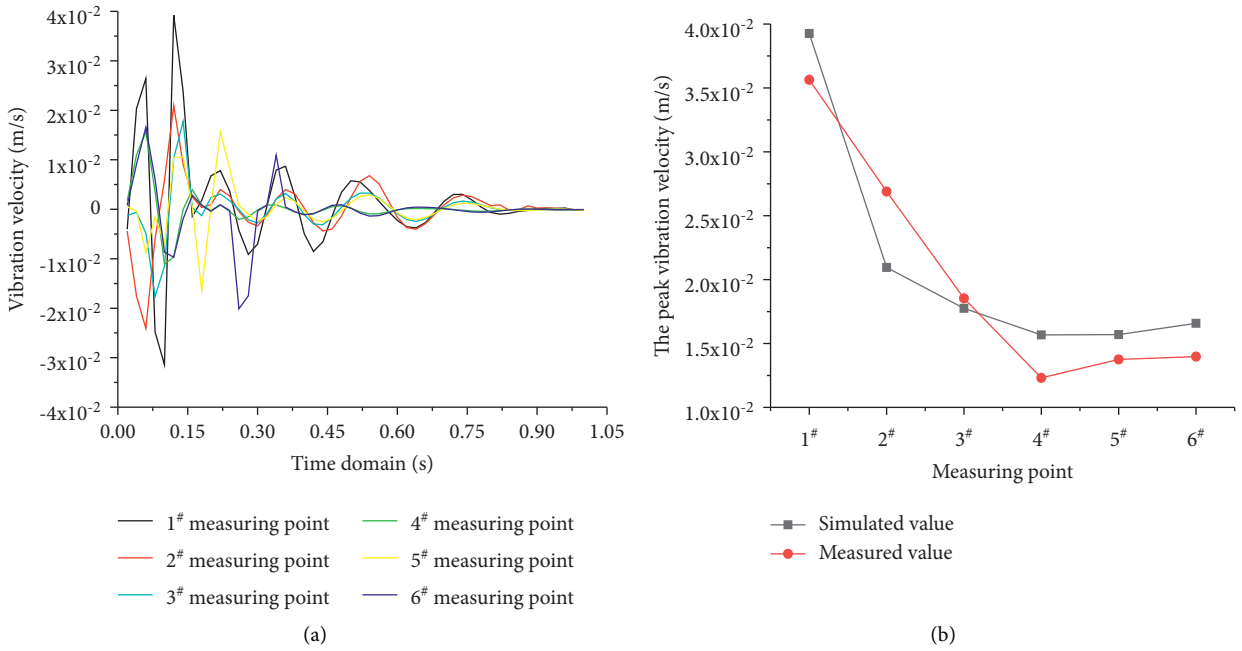

Figure 9: Comparison and verification of numerical simulation results. (a) Time-history curve of vibration velocity of each monitoring point in the model and (b) comparison curve of measured-simulated peak vibration velocity.

Table 5: Numerical simulation results of vibration data.

Monitoring point	Blasting center distance R (m)	Peak vibration velocity V (m/s)	Main vibration frequency f (Hz)	Amplitude A (m)
$1^{\#}$	10	3.926×10^{-2}	32.19	2.745×10^{-4}
$2^{\#}$	30	2.295×10^{-2}	25.76	1.831×10^{-4}
$3^{\#}$	65	1.775×10^{-2}	27.46	1.455×10^{-4}
$4^{\#}$	85	1.567×10^{-2}	20.28	1.739×10^{-4}
$5^{\#}$	120	1.57×10^{-2}	27.59	1.281×10^{-4}
$6^{\#}$	125	1.658×10^{-2}	39.2	9.520×10^{-5}

4. Prediction of Pre-Penetrating Surrounding Rock Vibration Velocity in Succeeding Tunnel

When the explosive explodes, the energy is released in the form of shock wave with high temperature (3000°C) and high pressure (10~100 Gpa) within about 3 ~ 7 times the radius of the charge from the explosion source firstly [43], as the blasting center distance increases to 120~150 times the charge radius, and the shock wave transforms into a compressive stress wave. When it exceeds 150 times the charge radius, the compressive stress wave will decay into a periodic vibration seismic wave [44], and the attenuation rate and action range of these three waveforms are different. If the shock wave and stress wave have a large intensity, which leads to plastic damage or even breakage of surrounding rock, it will not cause damage to surrounding rock until it is transformed into seismic wave, but only cause elastic vibration [45]. The surrounding rock in the pre-penetration area of the succeeding tunnel is far away from the blasting center. Therefore, the surrounding rock of the tunnel is mainly affected by seismic wave during the blasting process. The vibration velocity of the surrounding rock is proportional to the stress produced by blasting, so the vibration velocity can directly reflect the energy input from the seismic wave to the structure, and it provides a way to measure the stress change in the surrounding rock. The propagation of seismic waves in rock media is often affected by multiple factors, including the damping effect generated by the internal structure of the rock and the scattering reaction caused by its inhomogeneity, and all the above can lead to the consumption of blasting seismic wave and energy; at the same time, the vibration velocity will continue to decay.

4.1. Theoretical Analysis of Vibration Velocity of Tunnel Surrounding Rock. During the tunnel construction, the explosive will disturb the surrounding rocks and soil media at the moment of explosion, and there will be waves radiating in all directions from the blasting point. The blasting seismic waves can be approximately regarded as plane waves at a distance from the disturbance center. The simplest explanation for the problem of seismic wave absorption is assuming that the relative decrease in wave energy is

proportional to the distance traveled by the wave. Under the influence of the internal structure of surrounding rock and other factors, the energy in the process of seismic wave propagation decreases continuously, and the energy consumed is proportional to the propagation distance [3, 45, 46], namely,

$$E = E_0 e^{-2\beta r}. \tag{9}$$

In the equation:

E = the energy when the seismic wave propagation distance is r (m^2/s^{-2})

E_0 = the initial energy (energy at the source when the propagation distance of seismic wave tends to zero)

r = seismic wave propagation distance (m)

β = seismic wave absorption coefficient

The energy generated by tunnel blasting is proportional to the square of the vibration velocity of the surrounding rock.

$$E_e = cv^2 r^2. \tag{10}$$

According to formulas (9) and (10):

$$cv_r^2 r^2 = E_0 e^{-2\beta r}, \tag{11}$$

where the initial energy of seismic wave E_0 is as follows:

$$E = \eta E_e. \tag{12}$$

In the equation: η = coefficient; it can be calculated by formula $\eta = (k \cdot 10^{-2})^{3/\alpha} 10^{-3}$ [47, 48], and formula (13) can be obtained by substituting it into formulas (11) and (12).

$$E = cv_r^2 r^2 = \left(k \cdot 10^{-2}\right)^{3/\alpha} 10^{-3} E_e e^{-2\beta r}. \tag{13}$$

When r tends to 0, the seismic wave energy $E = cv_0^2$, where v_0 is the initial vibration velocity when the seismic wave is generated (which can be approximately regarded as the vibration velocity of the rock mass at the explosion source), and it is substituted into formula (13), namely,

$$v_r^2 r^2 = \left(k \cdot 10^{-2}\right)^{3/\alpha} 10^{-3} e^{-2\beta r} v_0^2 r_0^2. \tag{14}$$

The formula of peak vibration velocity at a certain blasting center distance can be obtained by simultaneously calculating square root on both sides of formula (14):

$$v_r = \frac{\left(k \cdot 10^{-2}\right)^{3/(2\alpha)} 10^{-3/2} e^{-\beta r} v_0 r_0}{r}. \tag{15}$$

In equation (15), k, α, and β can be derived from the monitoring data of the tunnel blasting project, and the formula can predict the vibration velocity of surrounding rock particles where the actual monitoring cannot be carried out and can be applied to evaluate the blasting effect under known blasting conditions.

Fitting calculation of k, α, and β coefficients is as follows.

(1) The coefficients k and α are fitted and calculated by Sadovsky's empirical equation:

$$v_r = k\left(\frac{Q^{1/3}}{r}\right). \tag{16}$$

In the equation:

k = coefficient related to propagation medium and blasting conditions
Q = the maximum charge of a single stage in delayed blasting (kg)
R = distance from blasting center (m)
V = blasting particle vibration velocity (m/s)
α = vibration attenuation coefficient, related to geological and topographic conditions and the distance from the blasting center

(2) The absorption coefficient β is related to the amplitude [49, 50]:

$$\beta = -\frac{\mathrm{d}}{\mathrm{d}r} \ln [A(r)r]. \tag{17}$$

In the equation:

A = amplitude of blasting seismic wave (m)

Formula (15) is generally applicable to all kinds of tunnel blasting excavation projects, but the coefficients k, α, and β are related to the actual geological and topographic conditions, explosive charge, blasting center distance, amplitude, and other factors of a certain tunnel project. By fitting and calculating the coefficients k, α, and β according to the actual project monitoring data, the prediction formula of characteristic vibration velocity applicable to this tunnel can be obtained. When applied to this tunnel project, the peak vibration velocity v_0 of the pre-penetration surrounding rock of the succeeding tunnel can be calculated, and then, the influence of the blasting construction of the preceding tunnel on the succeeding tunnel can be judged.

4.2. Determination of Peak Vibration Velocity of Tunnel Pre-Penetrating Surrounding Rock. According to the actual blasting monitoring situation and numerical simulation results of Kaifeng Mountain tunnel (Tables 4 and 5), the corresponding unknowns k, α, and β in the vibration velocity formula (15) are calculated using the above derivation process, and then, the formula is applied and verified.

Combined with Sadovsky's empirical equation (16) in Section 4.1, the data of total charge, blasting center distance, and particle vibration velocity obtained from the actual blasting and simulation result are analyzed. Then, the reduced distance $Q^{1/3}/R$ in (16) (the maximum charge Q of a single section of this project is 15.6 kg) is taken as the x-axis, the peak vibration velocity v of the monitoring points is taken as the y-axis to establish a coordinate system, and the relationship curve is drawn between the reduced distance and the vibration velocity, as shown in Figure 10(in the Figure: V = peak vibration velocity; $Q^{1/3}/R$ = reduced distance).

It can be seen from Figure 10 that the relationship between the reduced distance and the vibration velocity obtained from the actual engineering monitoring is

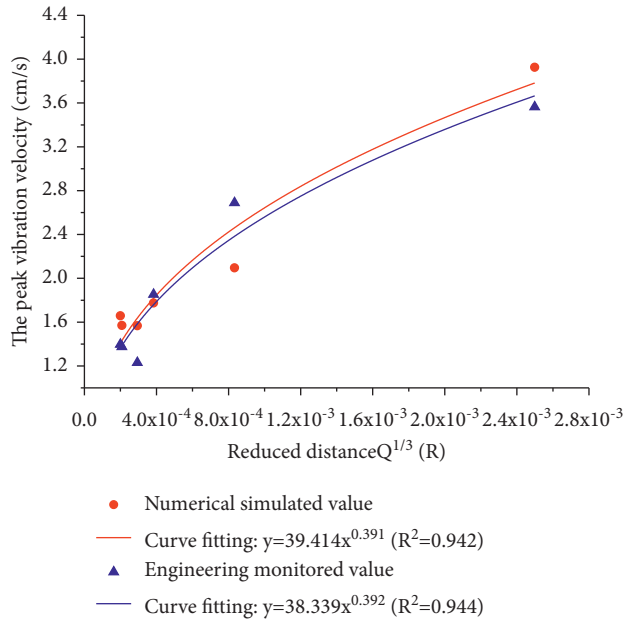

Figure 10: Relationship between the reduced distance and the vibration velocity.

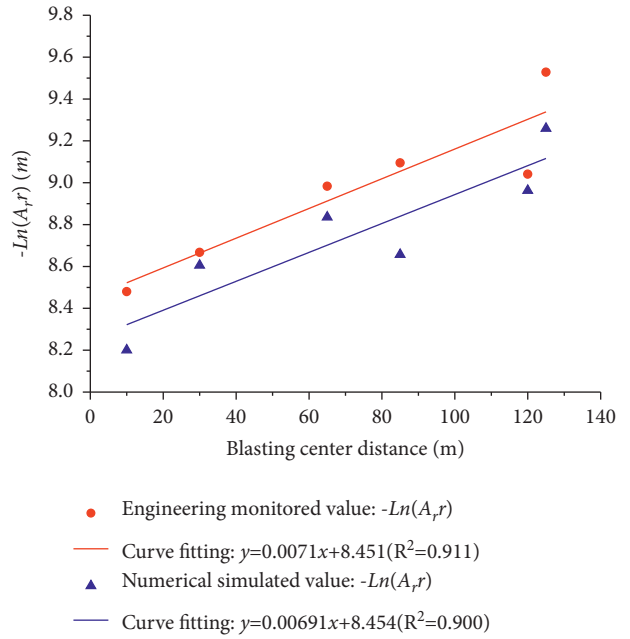

Figure 11: Solving diagram of seismic wave absorption coefficient.

$y = 38.339x^{0.392}$, and the correlation coefficient $R^2 = 0.944$; the relationship between numerical simulation reduced distance and vibration velocity is $y = 39.414x^{0.296}$, and the correlation coefficient $R^2 = 0.942$; the difference between the curve and formula fitted by them is very slight, which indicates that the fitting effect is well. Therefore, the fitting result obtained from the actual engineering monitoring with relatively high correlation coefficient will be more suitable for this tunnel engineering, with the coefficient k of 38.339 and the vibration attenuation coefficient α of 0.392.

In (15), the seismic wave absorption coefficient β still needs to be solved. (17) is combined to analyze the amplitude and the detonation center distance, and the relevant curve is drawn, as shown in Figure 11 (in the figure: A = amplitude; R = blasting center distance). The x-axis is the distance between the monitoring point and the explosion source (the blasting center distance r). The y-axis is $-Ln(A)$. The fitting formula obtained from actual engineering monitoring is $y = 0.0071x + 8.451$, and the correlation coefficient $R^2 = 0.911$; the fitting formula obtained by numerical simulation is $y = 0.00691x + 8.454$, and the correlation coefficient $R^2 = 0.900$; and the slope of the fitting curve is the seismic wave absorption coefficient β, and the seismic wave absorption coefficient β is 0.0071 when the fitting value of engineering monitoring is taken.

Combined with the coefficients k, α, and β obtained by fitting the above monitoring data and simulating result, the particle vibration velocity v_r in the seismic wave propagation process of the tunnel engineering can be obtained:

$$v_r = \left(38.339 \times 10^{-2}\right)\frac{3}{2 \times 0.392}10^{-\frac{3}{2}}e^{-0.0071r}\frac{v_0 r_0}{r} = 0.00080684e^{-0.0071r}\frac{v_0 r_0}{r}. \quad (18)$$

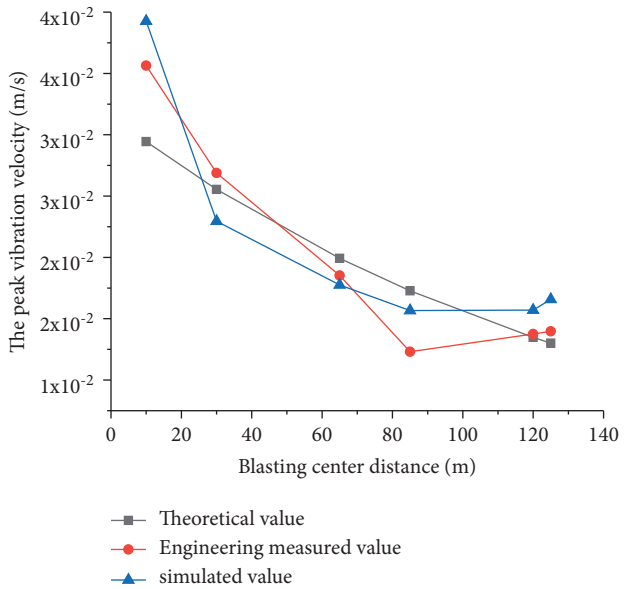

Figure 12: Theoretical-measured-simulated value error analysis.

The theoretical vibration velocity of 1#~6# measuring points can be calculated by theoretical derivation formula (18) and compared with the actual vibration velocity obtained by monitoring and simulating (Figure 12) (in the figure: v = peak vibration velocity; r = blasting center distance). It can be seen from the figure that the deviation among the theoretical value, the actual monitoring value, and the numerical simulation value is very slight, and all show a decreasing trend with the increase in blasting center distance, showing the same law basically, so the above theoretical derivation formula can play a certain role in predicting some special unmeasurable points on the surrounding rock.

The initial velocity v_0 is the same during blasting, which is difficult to monitor. To study the vibration velocity of each particle in the surrounding rock of the succeeding tunnel, the vibration velocity v_r of each particle in the process of seismic wave propagation is divided by the initial velocity v_0 to obtain the ratio χ, which is defined as the seismic wave vibration velocity ratio, namely,

$$\chi = \frac{v_r}{v_0} = \frac{\left(38.339 \times 10^{-2}\right)^{3/2\times 0.392} \times 10^{-3/2} e^{-0.0071r} r_0}{r} = \frac{0.00080684 e^{-0.0071r} r_0}{r}. \tag{19}$$

According to (19), the seismic wave vibration velocity ratio χ of derivation point can be calculated to reflect the vibration velocity change in surrounding rock in the pre-penetration area of the succeeding tunnel, and then, the influence of blasting vibration of the preceding tunnel on the vibration at any position of the succeeding tunnel can be obtained. Combined with the calculated seismic wave velocity ratio χ of each derivation point, a coordinate system with the blasting working face as y-axis and the blasting excavation direction of the tunnel as x-axis (Figure 5) is established. A curve graph is drawn according to the seismic wave velocity ratio χ of each theoretical calculation point changes with its location, as shown in Figure 13.

From the analysis in Figure 13, it can be seen that the closer the location of the derivation point is to the origin coordinate system, the seismic wave velocity ratio χ is greater; otherwise, it becomes smaller and smaller. When the abscess value is 0, it will reach the maximum value; that is, the surrounding rock section in the pre-penetration area corresponding to the blasting face is the most unfavorable section. It shows that the closer to the blasting working face, the vibration velocity of the surrounding rock and the disturbance are greater. In addition, by comparing the vibration velocity ratio χ of the derivation points on the front blasting side and the back blasting side, the χ value of the front blasting side is larger than the back blasting side. As the distance between the derivation points and the original point becomes further and further, the difference between the two derivation points becomes smaller and smaller. It shows that the impact of vibration velocity on the front blasting side of pre-penetration surrounding rock of the succeeding tunnel is greater than that on the back blasting side, and the influence on both sides gradually becomes consistent with the increase in distance.

Due to the limitation of construction conditions, the monitoring points and monitoring times that can be arranged are limited. At the same time, the stress redistribution and the failure pattern of surrounding rock in the pre-penetration area cannot be obtained completely through on-site monitoring. So, a numerical simulation calculation study is further conducted, which can deeply explore the variation of the plastic zone of the middle rock wall during the preceding tunnel blasting and the stress distribution of the surrounding rock in the pre-penetration area of the succeeding tunnel.

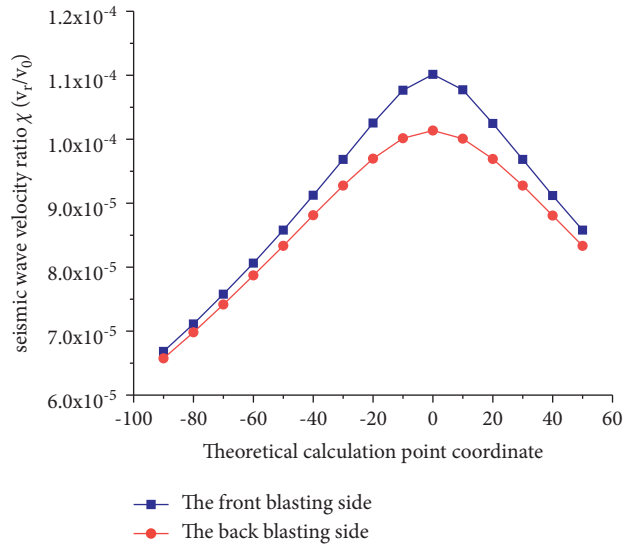

Figure 13: Variation curve of proportional coefficient χ.

5. Numerical Simulation Calculation and Analysis of Engineering Construction

In the simulation calculation, the same upper and lower step methods are used as the actual project, and the distance between the upper and lower step working face is 10 meters. Only the most unfavorable section in the conclusions obtained from the analysis of the theory and monitoring results for analysis are taken, and the model has a total of 8 monitoring points arranged along its pre-excavation contour line. The measuring points at the top and bottom of the arch are $1^{\#}$ and $8^{\#}$, the arch shoulders are $2^{\#}$ and $3^{\#}$, the arch waist is $4^{\#}$ and $5^{\#}$, and the arch feet are $6^{\#}$ and $7^{\#}$. The specific layout is shown in Figure 14.

5.1. Vibration Velocity Analysis. The simulated vibration velocity data are drawn into the maximum vibration velocity envelope diagram (Figure 15), and the vibration velocity comparison diagram of surrounding rock in the pre-penetration area of the succeeding tunnel when the upper and lower steps of the preceding tunnel are excavated is drawn (Figure 16).

Through Figure 15, it is found that the maximum vibration velocity always appears at the $5^{\#}$ measuring point, which is the arch waist, and the vibration velocity of other measuring points gradually decreases from arch waist⟶ arch shoulder⟶ arch foot⟶ arch top (bottom). As the clear distance gradually increases, the vibration velocity at the same position gradually decreases, and the area formed by the envelope diagram becomes smaller and smaller. It shows that with the increase in the tunnel clear distance, the impact of blasting vibration on the surrounding rock of the pre-penetration area becomes smaller and smaller.

According to Figure 16, the maximum vibration velocity of the measuring points on the front blasting side ($1^{\#}$, $3^{\#}$, $5^{\#}$, $7^{\#}$, and $8^{\#}$) and the back blasting side ($2^{\#}$, $4^{\#}$, and $6^{\#}$) is compared and analyzed and found that under the same clear distance condition the vibration velocity of the front blasting

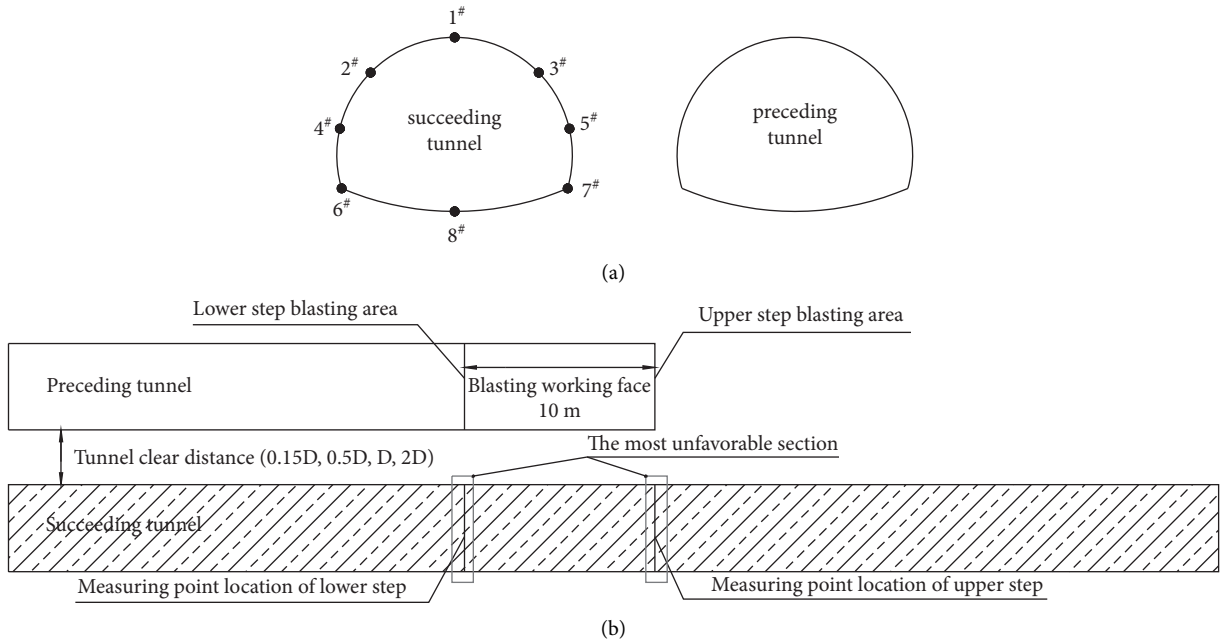

Figure 14: Schematic diagram of measuring point layout. (a) The position of the cross section of the measuring point and (b) plane position of measuring point.

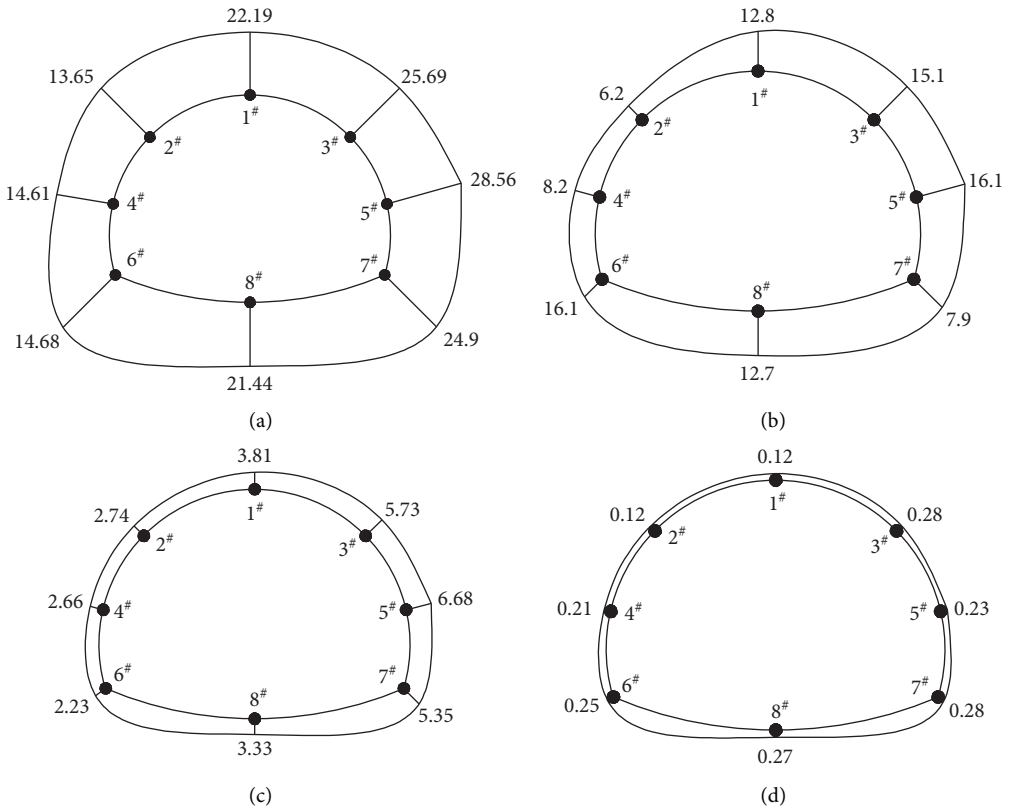

Figure 15: Tunnel vibration velocity envelope diagram. (a) Tunnel clear distance 0.15D, (b) tunnel clear distance 0.5D, (c) tunnel clear distance D, and (d) tunnel clear distance 2D.

side is greater than that of the back blasting side, and the variation range is larger, so the graph line is saw-toothed, and this is consistent with the law of on-site monitoring data. With the increase in the clear distance, the graph line gradually tends to a straight line, indicating that the surrounding rock can consume part of the energy generated by

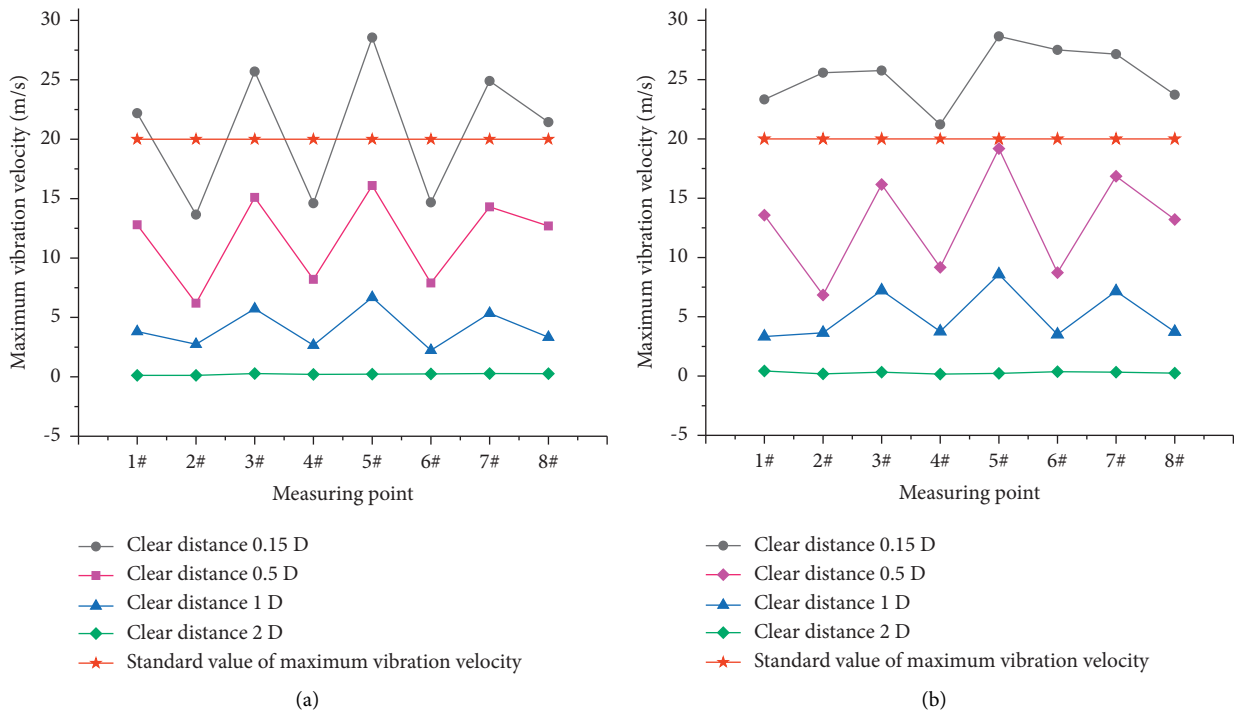

Figure 16: Vibration velocity of each measuring point under different clear distance conditions. (a) Excavated by upper step and (b) excavated by lower step.

blasting, thus reducing the vibration velocity. Comparing the vibration velocity of the same measuring point under different clear distance conditions, it is found that due to the vibration damping effect produced by the surrounding rock, the larger the clear distance, the smaller the maximum vibration velocity. According to the requirements of "*GB 6722-2014 Blasting Safety Regulations,*" the maximum allowable particle vibration velocity of tunnel blasting is 0.2 m/s, and when the tunnel clear distance is 0.15D, the measuring points at the side facing the blasting during the excavation of the upper step in the succeeding tunnel and the eight measuring points during the excavation of the lower step all exceed the specification requirements. It shows that if the clear distance is too small, the blasting vibration of the preceding tunnel will easily affect the stability of the surrounding rock in the pre-penetration area of the succeeding tunnel, so when the succeeding tunnel is excavated, the corresponding reinforcement measures should be taken in advance. All the measuring points with the tunnel clear distance greater than or equal to 0.5D meet the specification requirements, so the tunnel clear distance of 0.5D can be used as a dividing line of safety clear distance. Under the same clear distance condition, the vibration velocity of the tunnel at the same position when the lower step is excavated is greater than that when the upper step is excavated.

5.2. Plastic Strain Analysis. When the surrounding rock is destroyed, the plastic deformation and displacement on the failure surface will suddenly change. Therefore, the maximum point of plastic strain in each section of the surrounding rock is connected into a line, and the potential failure surface of the surrounding rock can be obtained, to judge the stability of the surrounding rock.

Figures 17–20 show the distribution of plastic strain in the rock wall and pre-penetration surrounding rock of the succeeding tunnel when the preceding tunnel is excavated under different clear distance conditions, in which the black line segment is the potential plastic failure surface. Through analysis, no matter what the clear distance of the tunnel is, the plastic strain area generated by the excavation of the upper step in the preceding tunnel tends to develop toward the arch top, and the plastic strain area generated by the excavation of the lower step tends to develop toward the arch bottom. When the clear distance is 0.15D, the middle rock wall and the surrounding rock of pre-penetration area of the succeeding tunnel all enter plastic state, and the potential failure surface of plastic strain is particularly obvious when the lower step is excavated, which is U-shaped and has a large distribution range. The results show that when the clear distance is 0.15D, the pre-penetration surrounding rock and the middle rock wall will be disturbed greatly, so the pre-reinforcement measures should be taken before the blasting of the succeeding tunnel. With the increase in clear distance, the plastic strain area and potential failure surface gradually become smaller and move away from the middle rock wall; that is, the influence of blasting excavation of the preceding tunnel on the middle rock wall and the surrounding rock of the succeeding tunnel is smaller and smaller. When the clear distance is greater than or equal to D, the surrounding rock in the pre-penetration area of the succeeding tunnel always maintains a state of elastic. So, according to the change law of plastic strain, D can be judged as the minimum safe clear distance.

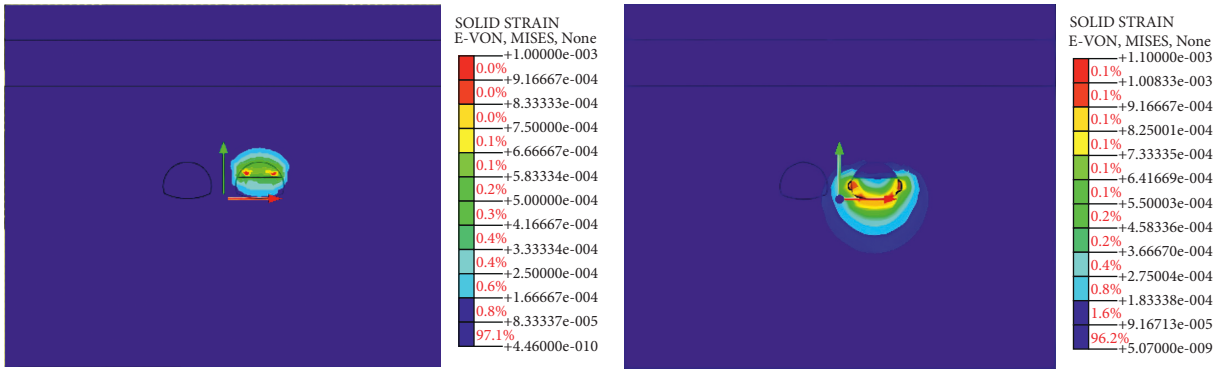

(a) (b)

Figure 17: Plastic strain distribution (tunnel clear distance 0.15D). (a) Excavation of upper step and (b) excavation of lower step.

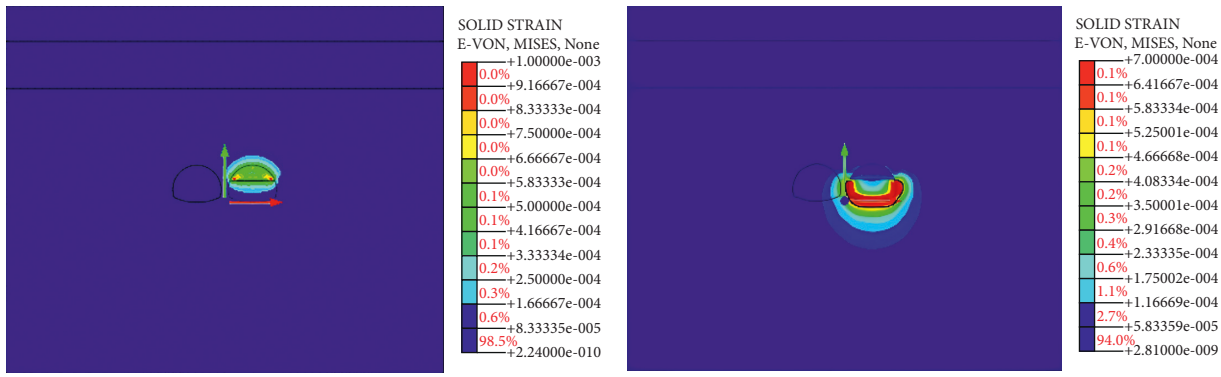

(a) (b)

Figure 18: Plastic strain distribution (tunnel clear distance 0.5D). (a) Excavation of upper step and (b) excavation of lower step.

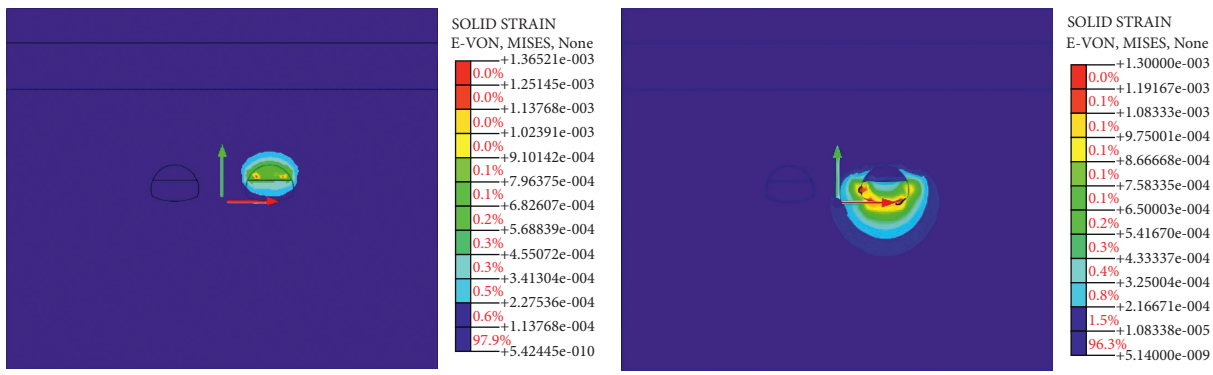

(a) (b)

Figure 19: Plastic strain distribution (tunnel clear distance D). (a) Excavation of upper step and (b) excavation of lower step.

5.3. Stress Analysis. To further study the stress distribution of the surrounding rock in the pre-penetration of the succeeding tunnel when the preceding tunnel is blasting, the stress distribution during the blasting of upper and lower steps of the preceding tunnel under different clear distance conditions is analyzed, as shown in Figures 21–24.

From Figures 21–24, it is found that the stress of surrounding rock is concentrated mostly around the surrounding rock of the preceding tunnel, and the distribution range expands with the increase in the clear distance of the tunnel, gradually moves away from the middle rock wall and the pre-penetration area of the succeeding tunnel, and tends to a safe and stable state. When the upper step is excavated, the maximum stress of the surrounding rock in the pre-penetration area of the succeeding tunnel is mainly distributed around the

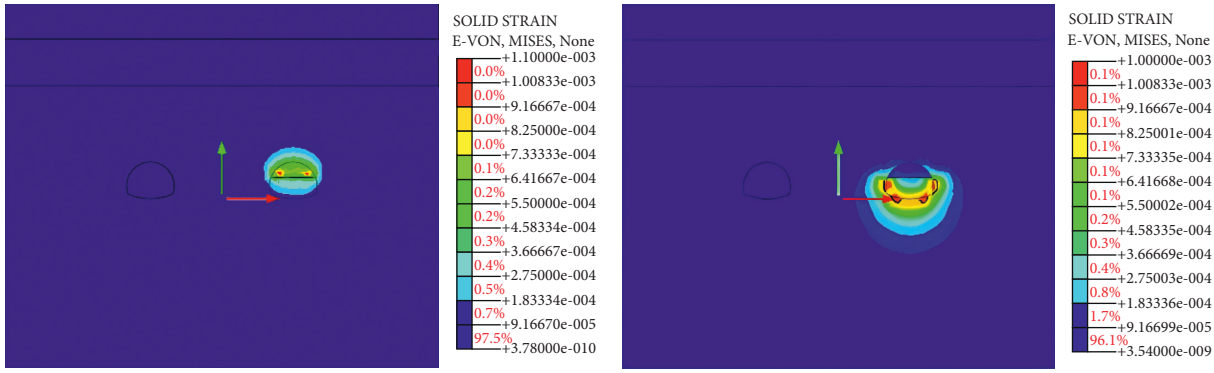

(a) (b)

Figure 20: Plastic strain distribution (tunnel clear distance 2D). (a) Excavation of upper step and (b) excavation of lower step.

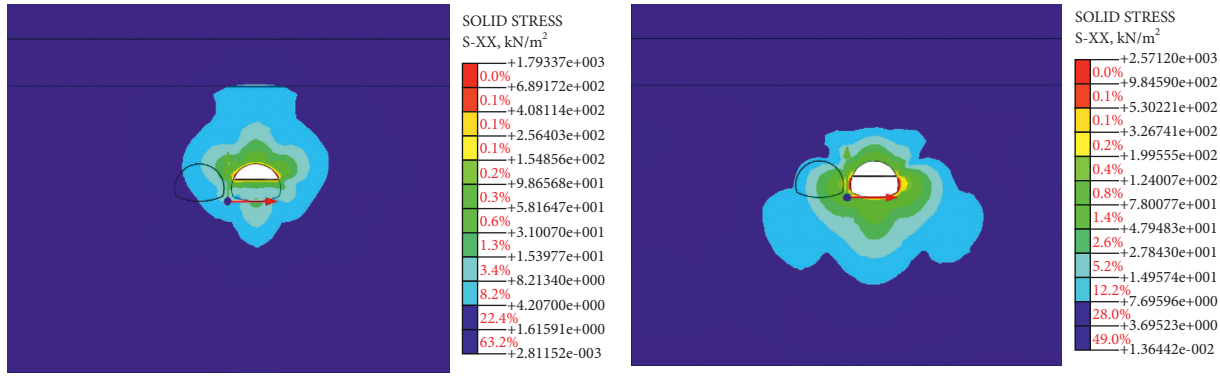

(a) (b)

Figure 21: Stress distribution of surrounding rock (tunnel clear distance 0.15D). (a) Excavation of upper step and (b) excavation of lower step.

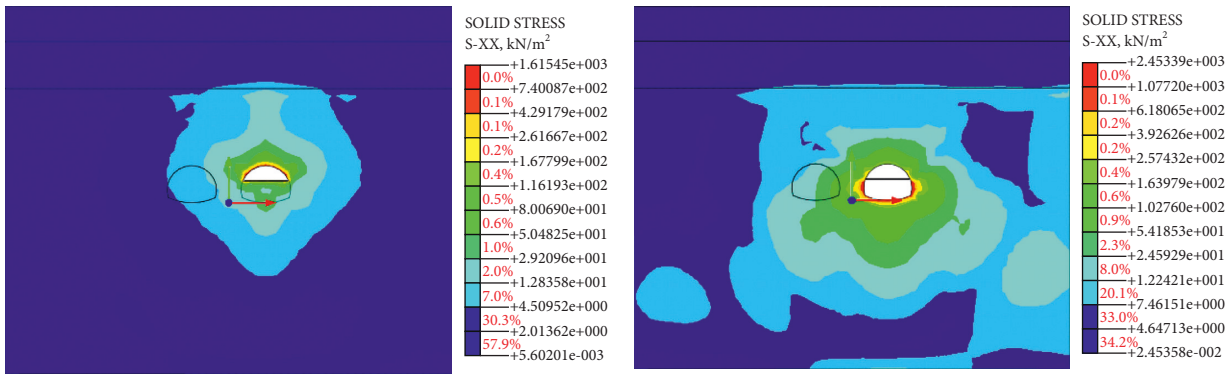

(a) (b)

Figure 22: Stress distribution of surrounding rock (tunnel clear distance 0.5D). (a) Excavation of upper step and (b) excavation of lower step.

excavation contour line of the upper step, and when the clear distance is 0.15D and 0.5D, the stress values of most of the middle rock wall and surrounding rock in the pre-penetration area of the tunnel are less than the tensile strength of the rock (the reference value of the tensile strength of the IV grade surrounding rock obtained from the tunnel geological survey is $0.2 \times 10^6 \sim 0.5 \times 10^6$ Pa; according to literature studies [38, 51–56], the dynamic tensile strength of rock changes little with the change in loading strain rate, while the shape and strain rate of Kaifeng Mountain tunnel after rock failure are not more than $10^3 s^{-1}$, which is within the range of loading strain

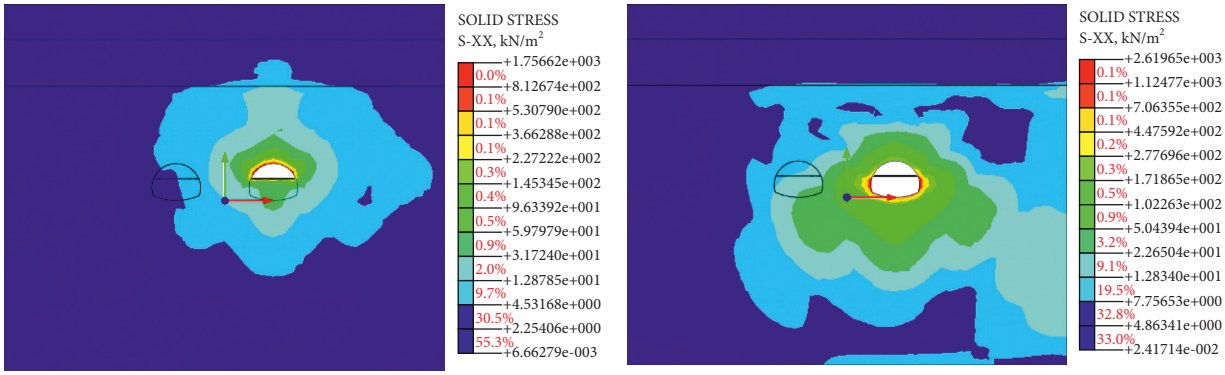

(a) (b)

FIGURE 23: Stress distribution of surrounding rock (tunnel clear distance D). (a) Excavation of upper step and (b) excavation of lower step.

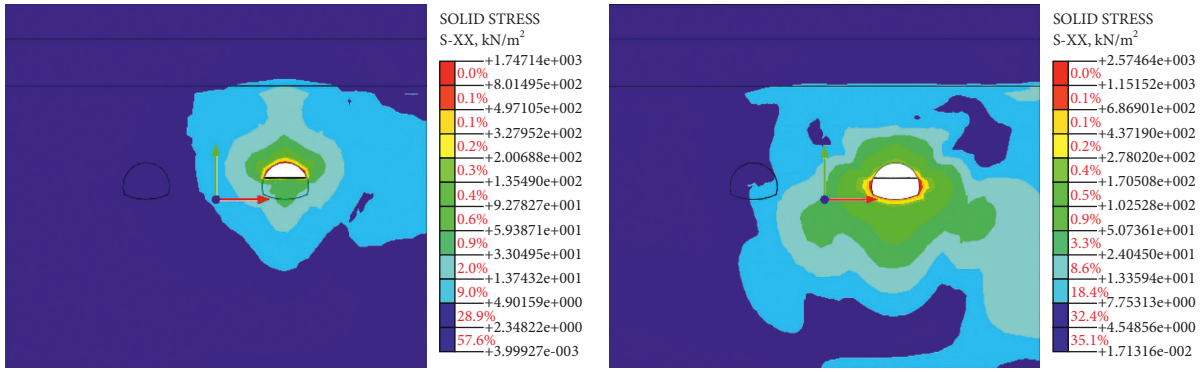

(a) (b)

FIGURE 24: Stress distribution of surrounding rock (tunnel clear distance 2D). (a) Excavation of upper step and (b) excavation of lower step.

rate of rock blasting. Therefore, the static tensile strength of rock mass is used to approximately replace the uniaxial dynamic tensile strength of rock mass in simulation), and the surrounding rock will not cause the type of tensile failure in this condition. When the lower step is excavated, the maximum stress of the pre-penetration surrounding rock is mainly distributed around the arch bottom of the lower step, and the stress distribution range is relatively large. The stress value of the whole middle rock wall and most of the pre-penetration surrounding rock of the tunnel with a clear distance of 0.15D is greater than the tensile strength of the rock, and the surrounding rock is prone to tensile failure. While in the tunnel with a clear distance of 0.5D, the half range of the front blasting side of the middle rock wall is the tensile failure area. When the clear distance of the tunnel is greater than or equal to D, the stress values of all middle rock wall and the surrounding rock of the succeeding tunnel are less than the tensile strength of the rock. The surrounding rock of the tunnel is in a stable state and will not be destroyed, so D is the safe clear distance [57].

6. Conclusions

(1) According to theoretical derivation and field monitoring analysis, it is concluded that the peak vibration velocity is negatively correlated with the blasting center distance of the preceding tunnel; the larger the distance, the smaller the vibration velocity, the smaller the seismic wave velocity ratio, and the smaller the disturbance to the surrounding rock. The surrounding rock on the front blasting side is more affected by blasting vibration than that at the back blasting side of the succeeding tunnel, and the section of the pre-penetration area of the succeeding tunnel parallel to the blasting working face of the preceding tunnel is the most unfavorable.

(2) Through the analysis of the vibration velocity of the numerical simulation, it is found that the vibration velocity of the front blasting side at the same position is greater than that of the back blasting side, and the vibration velocity gradually decreases from arched waist⟶ arched shoulder⟶arched foot⟶arch top (bottom), which is consistent with the law obtained from field monitoring. With the gradual increase in the clear distance, the variation range of vibration velocity between each measuring point decreases, and the impact of blasting vibration on the surrounding rock in the pre-penetration area becomes smaller and smaller.

(3) Under the same clear distance conditions, compared with the stress value and the range of plastic area in the rock wall and the pre-penetration surrounding rock of the succeeding tunnel, it is found that the lower step excavation is larger than that of the upper step excavation of the preceding tunnel, and the disturbance and failure of the pre-penetration surrounding rock and the middle rock wall are stronger. With the increase in the clear distance, the disturbance effect of the blasting of the preceding tunnel on the succeeding tunnel gradually decreases until both the middle rock wall and the pre-penetration surrounding rock reach a stable state.

(4) By analyzing the change law of the maximum vibration velocity, it is found that all measurement points meet the specification requirements when the clear distance of the tunnel is greater than or equal to 0.5D. It is found that when the clear distance is greater than or equal to D, the excavation of the preceding tunnel will not affect the middle rock wall and the pre-penetration surrounding rock of the succeeding tunnel by analyzing the stress distribution and plastic strain. Therefore, based on the research results of three aspects, it is concluded that the minimum safe clear distance is D.

(5) From the prediction formula of vibration velocity, it is found that the vibration velocity of surrounding rock in tunnel blasting construction is mainly related to geological and topographic conditions, explosive charge, blasting center distance, amplitude, and other factors. Through the actual engineering monitoring and the fitting calculation and mutual verification of numerical simulation data, it shows that this theory can be well applied to the corresponding tunnel, can predict the maximum vibration velocity of surrounding rock in the pre-penetration area, and can well guide the engineering construction, which can provide a reference for similar projects.

Data Availability

The data used to support the findings of this study are included within the article.

Conflicts of Interest

The authors declare that there are no conflicts of interest regarding the publication of this study.

Acknowledgments

The study was supported by Inner Mongolia Natural Science Foundation (grant no. 2020LH05018), Inner Mongolia Natural Science Foundation (grant no. 2019MS05053), Inner Mongolia University of Science and Technology Institute of Building Science Open Foundation (grant no. JYSJJ-2021M19), and Inner Mongolia Natural Science Foundation (grant no. 2020BS05017).

References

[1] X. X. Tian, Z. P. Song, and J. B. Wang, "Study on the propagation law of tunnel blasting vibration in stratum and blasting vibration reduction technology," *Soil Dynamics and Earthquake Engineering*, vol. 126, Article ID 105813, 2019.

[2] W. B. Lu and W. Hustrulid, "An improvement to the equation for the attenuation of the peak particle velocity," *Engineering Blasting*, vol. 8, no. 3, pp. 1–4, 2002.

[3] H. T. Li, W. B. Lu, D. Q. Shu, X. G. Yang, and C. P. Yi, "Study of energy attention law of blast-induced seismic wave," *Chinese Journal of Rock Mechanics and Engineering*, vol. 29, no. 1, pp. 3364–3369, 2010.

[4] J. H. Yang, W. B. Lu, M. Chen, P. Yan, and C. B. Zhou, "Microseism induced by transient release of in situ stress during deep rock mass excavation by blasting," *Rock Mechanics and Rock Engineering*, vol. 46, no. 4, pp. 859–875, 2013.

[5] H. L. Fei, X. Y. Zeng, and Z. G. Yang, "Influence of tunnel excavation blasting vibration on earth's surface based on wavelet packet analysis," *Explosion and Shock Waves*, vol. 37, no. 1, pp. 77–83, 2017.

[6] W. W. Yao, S. Q. Yang, and J. Sun, "Research on rail vibration characteristics of railway tunnel under ultra-close blasting vibration," *Journal of Hunan University of Technology*, vol. 32, no. 6, pp. 14–20, 2018.

[7] R. L. Shan, Y. W. Song, Y. Bai, L. Z. Zhang, and T. Zhou, "Study on energy attenuation characteristics of blasting signal based on wavelet packet transform," *Mining Science Journal*, vol. 3, no. 02, pp. 119–128, 2018.

[8] R. P. Dai, X. B. Guo, Q. M. Gong, C. J. Pu, and Z. C. Zhang, "Shpe test on blasting damage protection of tunnel surrounding rock," *Rock and Soil Mechanics*, vol. 32, no. 01, pp. 77–83, 2011.

[9] P. Liu, X. Zhou, and Q. Qian, "Experimental investigation of rigid confinement effects of radial strain on dynamic mechanical properties and failure modes of concrete," *International Journal of Mining Science and Technology*, vol. 31, no. 5, pp. 939–951, 2021.

[10] X. C. Ji, H. X. Fu, H. Kong, and Y. F. Gao, "Study on Microvibration drilling and blasting of large span tunnel using small spacing and vibration characteristics of intermediate rock wall," *China Journal of Highway and Transport*, vol. 34, no. 04, pp. 220–230, 2021.

[11] Y. Fan, W. B. Lu, J. H. Yang, P. Yan, and M. Chen, "Attenuation law of vibration induced by transient unloading during excavation of deep caverns," *Rock and Soil Mechanics*, vol. 36, no. 2, pp. 541–549, 2015.

[12] S. Xu, R. Liang, F. T. Suorineni, and Y. H. Li, "Evaluation of the use of sublevel open stoping in the mining of moderately dipping medium-thick orebodies," *International Journal of Mining Science and Technology*, vol. 31, no. 2, pp. 333–346, 2021.

[13] S. Xu, T. Chen, J. Liu, C. Zhang, and Z. Chen, "Blasting vibration control using an improved artificial neural network in the ashele copper mine," *Shock and Vibration* no. 2, , pp. 2021–11.

[14] P. Jayawardana, D. P. Thambiratnam, N. Perera, and T. Chan, "Dual in-filled trenches for vibration mitigation and their predictions using artificial neural network," *Soil Dynamics and Earthquake Engineering*, vol. 122, pp. 107–115, 2019.

[15] X. P. Guo, S. J. Yang, Z. H. Zhu, Z. B. Xiang, Z. H. Zhang, and G. Q. Hu, "Prediction of blasting vibration velocity using GA-BP neural network," *Blasting*, vol. 37, no. 3, pp. 148–152, 2020.

[16] Y. Wang, *Prediction of Blasting Vibration Based on Artificial Neural Network and Random Forest*, MSc Thesis, Guangxi University, Nanning, China, 2020.
[17] M. Cardu, D. Coragliotto, and P. Oreste, "Analysis of predictor equations for determining the blast-induced vibration in rock blasting," *International Journal of Mining Science and Technology*, vol. 29, no. 6, pp. 905–915, 2019.
[18] L. He, D. W. Zhong, P. Li, K. Song, and J. F. Si, "Vibration prediction and energy analysis of slope under blasting load in underpass tunnel," *Explosion and Shock Waves*, vol. 40, no. 7, pp. 108–117, 2020.
[19] L. B. Jayasinghe, H. Y. Zhou, A. T. C. Goh, Z. Y. Zhao, and Y. L. Gui, "Pile response subjected to rock blasting induced ground vibration near soil-rock interface," *Computers and Geotechnics*, vol. 82, pp. 1–15, 2017.
[20] X. M. Liu and S. H. Chen, "Prediction of surface vibration waveform caused by cut hole blasting in tunnel excavation," *Chinese Journal of Geotechnical Engineering*, vol. 41, no. 9, pp. 1731–1737, 2019.
[21] F. Xie, L. Han, D. S. Liu, and C. Li, "Vibration law analysis for a tunnel's field near blasting based on wave form superposition theory," *Journal of Vibration and Shock*, vol. 37, no. 2, pp. 182–188, 2018.
[22] W. Q. Wu and K. K. Jin, "The study of relationship between surrounding rock strength, blasting vibration velocity and their influence on structure in small clear distance tunnel," *Highways*, vol. 61, no. 05, pp. 254–257, 2016.
[23] Y. Liu, *Study on Reasonable Distance and Construction Reinforcement Technology for Small-Distance Tunnels in Cities*, MSc Thesis, Southwest Jiaotong University, Chengdu, China, 2019.
[24] K. Yang, S. C. Wu, Q. L. Wu, W. C. Song, and Q. Z. Wang, "Cause analysis of a highway tunnel collapse and the treatment technology," *Chinese Journal of Underground Space and Engineering*, vol. 11, no. 1, pp. 239–245, 2015.
[25] D. M. Guo, K. Liu, W. Zhang, J. Yang, and L. F. Fan, "Research on failure rule and dynamic response of tunnel under adjacent blasting loads of different spacing," *Transactions of Beijing Institute of Technology*, vol. 38, no. 10, pp. 1000–1005, 2018.
[26] J. L. Li, J. G. Wu, and Q. Bi, "Study on the design and construction method for the large-span highway tunnel with small interval," *Modern Tunnelling Technology*, vol. 56, no. 5, pp. 157–162+227, 2019.
[27] H. L. Wang, J. Dang, Z. H. Wu, and Z. G. Wang, "Impact of undercrossing tunnel on safety and stability of existing heavy-duty railway tunnel," *Journal of the China Railway Society*, vol. 42, no. 6, pp. 102–111, 2020.
[28] X. M. Guan, L. Zhang, Y. W. Wang, H. X. Fu, and J. Y. An, "Velocity and stress response and damage mechanism of three types pipelines subjected to highway tunnel blasting vibration," *Engineering Failure Analysis*, vol. 118, Article ID 104840, 2020.
[29] R. Yang, L. Zhao, C. Han, W. Chen, and K. Guo, "Monitoring and control of construction blasting vibration of large-span tunnels with small clear spacing," *Construction Technology*, vol. 47, no. 1, pp. 711–714, 2018.
[30] L. Jia, Y. P. Xie, and S. K. Li, "Numerical simulation for impact of blasting vibration on nearby tunnel lining safety," *Journal of Vibration and Shock*, vol. 34, no. 11, pp. 173–177+211, 2015.
[31] MC. Liu, "Impact analysis on construction of large section and small spacing road tunne," *Journal of Shandong University*, vol. 49, no. 4, pp. 78–85, 2019.
[32] L. M. Zhang, Y. R. Zheng, Z. Q. Wang, and J. X. Wang, "Application of strength reduction finite element method to road tunnels," *Rock and Soil Mechanics*, vol. 28, no. 1, pp. 97–101+106, 2007.
[33] K. Wu, Z. Shao, and S. Qin, "An analytical design method for ductile support structures in squeezing tunnels," *Archives of Civil and Mechanical Engineering*, vol. 20, no. 3, p. 91, 2020.
[34] KH. Yu, *Study on the Influence of Expanding Excavation Blasting of Existing Parallel Adit on the Safety of Shanshutuo Tunnel*, MSc Thesis, Chongqing Jiaotong University, Chongqing, China, 2019.
[35] J. Lysmer and R. L. Kuhlemeyer, "Finite dynamic model for infinite media," *Journal of the Engineering Mechanics Division*, vol. 95, no. 4, pp. 859–877, 1969.
[36] V. Besharat, M. Davoodi, and M. K. Jafari, "Variations in ground surface responses under different seismic input motions due the presence of a tunnel," *Arabian Journal for Science and Engineering*, vol. 39, no. 10, pp. 6927–6941, 2014.
[37] T. Y. Song, S. H. Wang, M. F. Wan, Y. Liang, and W. J. Rao, "Stability analysis on surrounding rock of small spacing tunnel under blasting construction," *Chinese Journal of Underground Space and Engineering*, vol. 9, no. 02, pp. 380–386+391, 2013.
[38] C. Luo, X. A. Yang, D. H. Luo, and H. Q. Zhang, "An improved tunnel blast simulation method and its verification," *Journal of Vibration and Shock*, vol. 38, no. 17, pp. 260–267, 2019.
[39] JT. Yang, *Study on Effect of Metro Station Blasting Construction on Building on the Ground*, MSc Thesis, Chongqing Jiaotong University, Chongqing, China, 2016.
[40] C. J. Konya and E. J. Walter, *Rock Blasting and over Break control*, National Highway Institute, Dwarka, Delhi, 1991.
[41] A. M. Starfield and J. M. Pugliese, "Compression waves generated in rock by cylindrical explosive charges: a comparison between a computer model and field measurements," *International Journal of Rock Mechanics and Mining Sciences & Geomechanics Abstracts*, vol. 5, no. 1, pp. 65–77, 1968.
[42] Y. T. Zhang, X. L. Ding, and S. L. Huang, "Field measurement and numerical simulation of excavation damaged zone in a 2000 m-deep cavern," *Geomechanics and Engineering*, vol. 16, no. 4, pp. 399–413, 2018.
[43] M. R. Zareifard, "A new semi-numerical method for elasto-plastic analysis of a circular tunnel excavated in a Hoek–Brown strain-softening rock mass considering the blast-induced damaged zone," *Computers and Geotechnics*, vol. 122, Article ID 103476, 2020.
[44] W. Zhang, *Analysis of Slope Stability and Elevation Effect under Blasting in Open-Pit Mine*, MSc Thesis, Taiyuan University of Technology, Taiyuan, China, 2017.
[45] J. Liu, J. Ba, J. W. Ma, and H. Z. Yang, "Seismic wave attenuation analysis in random porous media," *Scientia Sinica*, vol. 40, no. 07, pp. 858–868, 2010.
[46] J. Devine, R. Beck, A. Meyer, and W. Duvall, "Effect of charge weight on vibration levels from quarry blasting," *Report of Investigations 6774*, US Bureau of Mines, Washington, USA, 1966.
[47] F. P. Savarenski, Science Press, Beijing, Seismic wave[M]. Translated by DUAN Xingbei, 1981.
[48] S. Q. Zhang and J. M. Guo, "Calculation of energy conversion coefficient of explosive earthquake and application," *Chinese Journal of Geophysics*, vol. 27, no. 6, pp. 537–548, 1984.
[49] T. J. Tao, X. G. Wang, E. A. Chi, and J. H. Zhang, "Attenuation formula of blasting seismic wave based on energy theory," *Engineering Blasting*, vol. 21, no. 06, pp. 78–83, 2015.
[50] Z. M. He, J. Cai, F. Huang, and Y. X. Liu, "Analysis of influence of drilling and blasting construction on surrounding

rock damage of multi-arch tunnel based on energy method," *China Journal of Highway and Transport*, vol. 32, no. 9, pp. 143–151+182, 2019.

[51] S. Said and L. Auersch, "Prediction of explosion-induced ground and building vibrations - measured wave velocities, transfer functions and attenuation," in *Proceedings of the 25th International Congress on Sound and Vibration*, pp. 1–8, Hiroshima, 2018.

[52] S. H. Cho, Y. Ogata, and K. Kaneko, "Strain-rate dependency of the dynamic tensile strength of rock," *International Journal of Rock Mechanics and Mining Sciences*, vol. 40, no. 5, pp. 763–777, 2003.

[53] F. Dai and K. Xia, "Loading rate dependence of tensile strength anisotropy of barre granite," *Pure and Applied Geophysics*, vol. 167, no. 11, pp. 1419–1432, 2010.

[54] H. L. Fei, C. S. Zhao, C. Y. Yang, S. Q. Xiao, and G. J. Qu, "Damage range of tunnel surrounding rock under blasting load," *Engineering Blasting*, vol. 23, no. 06, pp. 1–4, 2017.

[55] J. Dai, *Dynamic Behaviors and Blasting Theory of Rock*, pp. 123–126, Metallurgical Industry Press, Beijing, 2002.

[56] X. Xia, "Study on damage characteristics and safety threshold of rock vibration by blast," Ph. D Thesis, Institute of Rock and Soil Mechanics, Chinese Academy of Sciences, Wuhan, 2006.

[57] L. Wu, W. B. Lu, and Q. Zong, "Distribution of explosive energy consumed by column charge in rock," *Rock and Soil Mechanics*, no. 05, pp. 735–739, 2006.